Design and characterization of liquid nanocapsules of rosemary oil (*Rosmarinus officinalis L.*)

Jesus Briones-Concha[a], Luz Irene Pascual-Mathey[b], César Ignacio Beristain[a] y Luz Alicia Pascual-Pineda[c]
[a]*Instituto de Ciencias Básicas,*
[b]*Facultad de Química Farmacéutica Biológica,*
[c]*Unidad de Servicios de Apoyo en Resolución Analítica (SARA),*
Universidad Veracruzana, Xalapa, México.
Email: lpascual@uv.mx

***Abstract*—Currently, plants are important to produce medicines and functional foods, as they are a source of bioactive compounds. One of the plants that have been investigated since ancient times is rosemary (*Rosmarinus Officinalis L.*). The essential oil of rosemary is a complex mixture of volatile compounds used in the food industry since it contains phenols, flavonoids, and terpenes. These molecules have antimicrobial, neuroprotective, antioxidant, and anti-inflammatory, as well as anti-tumor properties. Therefore, it is necessary to enhance the benefits that these bioactive compounds can provide through the production of nanoemulsions, which would increase the bioavailability and absorption of these. The main objective of the present work was to prepare and characterize oil/water (O/W) nanoemulsions of rosemary aqueous extract and essential oil elaborated by ultrasound. To achieve the nanoemulsions, the aqueous phase was to prepare by a liquid-solid extraction method (ratio 1:6), whereas 0.3% of essential oil as lipidic phase, using Tween 40 and Span 20 as surfactants. Nanoemulsions loaded with rosemary extracts were fabricated using surfactants blend with a hydrophilic-lipophilic balance (HLB), ranging from 10 to 14 with a high-power ultrasound. The analysis of the appropriate parameters was performed out by evaluating the particle size, zeta-potential and polydispersion index. The mean diameters (Z-average) of the dispersed particles containing rosemary extracts ranged from 50 to 437 nm and negative value of Z-potential. The results showed that the nanoemulsions with better characteristics are those of 12 HLB value and 1:1.5 oil: surfactant ratio. These results provide useful information for the design of delivery systems to encapsulate and stabilize lipophilic molecules.**

Keywords— rosemary, nanoemulsion, stability, particle size.

I. INTRODUCTION

Rosemary (*Rosmarinus Officinalis L.*) is a plant that has several compounds including phenols, flavonoids and terpenes, to which different biological activities have been attributed [1]. The carnosol is one of the main terpenoid bioactive compounds present in rosemary. The phenolic compounds include the carnosic acid, whose most abundant levels are in the leaves and the rosmarinic acid which is a natural compound that is currently a valuable product used in food, cosmetics and Pharmaceutical [1-2]. These three compounds have shown significant antioxidant activity reported in different studies [3]. In addition, other functions have been reported, such as antimicrobial, neuroprotective, and anti-inflammatory [4-5] as well as anti-tumor properties [6-9]. The most important by-product of this plant is the aqueous extract and the essential oils, which are used in the industry to improve the organoleptic and preservation qualities of foods [10]. This, in addition to the different biological activities previously reported, suggests to rosemary by-products as a possible candidate to prevent and/or treat some physiological alterations, including cancer. Therefore, it is necessary to enhance the benefits that bioactive compounds can provide through different systems. Additionally, these systems must be designed in order to achieve adequate dispersion in the food matrix, as well as adequate control in interaction with other ingredients, and the preservation of its activity during the storage time. Emulsions have proved to be a good option of encapsulation of lipophilic compounds. They are homogeneous systems composed of two immiscible liquid phases, one of them disperses as small droplets in the other, which can be of three types; conventional emulsions, nano and microemulsions, which have particle sizes of 100-1000, 10-100 and 2-10 nm, respectively [10-11]. Within those, nanoemulsions are highly stable, as they can generate greater thermodynamic stability derived from their small size and monodispersity, which may help to improve the protection of bioactive compounds and reduce the impact of essential oils on sensory properties and improve their biological activity [12-13]. Their physical stability implies that they can be diluted without changing the size distribution of droplet, being of great importance for the encapsulation of lipophilic functional components [11,14]. Also, highly lipophilic compounds have the advantage of being better solubilized into the gastrointestinal tract, favoring a better absorption of the bioactive compounds and therefore, their availability in the body [13]. Thus, the objective of this work was to develop and characterize oil-in-water nanoemulsions (O/W) of essential oil and aqueous extract of rosemary, measured through the evaluation of particle size, zeta-potential and polydispersion index (PDI).

II. METODOLOGY

A. Preparation of aqueous extract

The aqueous extract was made by a solid-liquid extraction in a ratio 1:6 dried sheet of rosemary: water at 100 ºC for 5 minutes. The extracted mixture was then filtered, centrifugated at 4750

The Mexican National Council for Science and Technology (CONACyT) funded this project CB-2015 25269.

978-1-7281-3304-1/19/$31.00 ©2019 IEEE

rpm at 4°C and the °Brix was measured to standardize the concentration of soluble solids. The supernatant was obtained and stored at 4°C.

B. Elaboration of emulsion

Emulsions were carried out according to the doses previously reported. The oil phase consisted of rosemary essential oil (AMCO), the aqueous phase to rosemary extract and the surfactant consisted of a mixture of Tween 40 (Polyoxyethylenesorbitan monopalmitate; Sigma-Aldrich; HLB 15.6) and Span 20 (Sorbitan monolaurate, Sigma-Aldrich; HLB 8.6) to determine the required hydrophilic-lipophilic balance a surfactants blend within the range value of 10 to 14 was used. The oil phase was prepared at 0.3% to get the dosing requirements of essential oil (10 mg/kg) previously reported [15]. Once the oil phase was fixed, four formulations were made to obtain v/v ratios of essential oil: surfactant to 1:1, 1:1.5, 1:2 and 1:3. The aqueous phase was adjusted to each relation: 99.4% in the 1:1 ratio; 99.25%, 99.1% and 98.8% in the 1:1.5, 1:2 and 1:3 ratios, respectively, meeting the dose of 200 mg/kg of aqueous extract reported by Al-Attar & cols. [16]. The rosemary essential oil was dispersed in an aqueous surfactant solution by a high-speed homogenizer (Wiggen Hause, Germany) at 13,000 rpm for 5 min to obtain the primary emulsion.

C. Preparation of the nanoemulsion

Subsequently, 30 mL of the primary emulsion was subjected to an ultrasonic processor of 20 kHz and a maximum power of 750 W Cole-Parmer instruments, model CPX 750, (USA), the sonication was carried out for 10 min at 30% of amplitude, the temperature was kept at 25º C by using an ice bath. These conditions are based on the previous experimental data obtained in our lab.

D. Analysis of particle size, PDI and zeta-potential

The particle size, zeta-potential and polydispersion index were analyzed in a Zetasizer (Malvern, Nano-ZS Worcestershire, UK) at 633 nm and 25°C. An aliquot of 20 µL of nanoemulsion was taken, to which 2 mL of injectable water were added and the measurements were carried out on the Zetasizer. Three replicates of each sample were analyzed to obtain the parameters. All obtained data were expressed as mean±standard deviation (M±SD).

III. RESULTS AND DISCUSION

A. Characterization of nanoemulsions

1) Effect of HLB and surfactant concentration of particle size nanoemulsions.

Table I shows the particle sizes expressed as particle diameter in nm. The mean diameter (Z-average) of the emulsions ranged between 50 and 478.3 nm; however, they not shown a consistent pattern of the effect of HLB and surfactant concentration. Their results showed that the nonionic surfactants could be used to produced rosemary emulsions with the dispersed droplets in the nanometric range. Colloidal systems with particle sizes <100 nm are considered nanoemulsions. McClements & Rao indicated that the drop size to consider an emulsion as nanoemulsion should be in the range of 10–100 nm, which could enhance the bioavailability of lipophilic compound [14]. A smaller particle size (50.03 nm) in the emulsion with oil: surfactant ratio of 1:1.5 wt/wt was obtained. In general, the smallest particle size was achieved with 12 HLB value. In this study, the smallest particle size was obtained at a ratio of 1:1.5 oil: surfactant, except for HLB of 14. This behavior indicates that a more moiety of the hydrophilic surfactant chain does not promote the decrease in the particle size. Walker & cols., observed in fish oil emulsions that at higher concentration of surfactant, the particle size decreases [17]; because more surfactant is necessary to cover more surface area. However, Jo & cols., reported, in cinnamaldehyde emulsions, that a greater amount of surfactant can form micelles and obtain larger particle sizes [18], which is consistent with this research since the high particle size was obtained at the highest surfactant concentration (1:3 wt/wt). Additionally, our results suggested that at oil: surfactant > 1:1.5 the droplets are completely covered by the emulsifier, whereas the surfactant excess is in the continuous phase.

TABLE I. EFFECT OF HLB AND SURFACTANT CONCENTRATION ON THE PARTICLE SIZE OF ROSEMARY NANOEMULSIONS

Oil/Surf ratio (wt/wt) HLB	**Particle size (nm)**			
	1:1	***1:1.5***	***1:2***	***1:3***
14	319.7±33.86	478.3±64.4	138.1±21.15	437.2±72.35
13	79.9±4.27	131.7±2.57	140.8±57.85	218.4±16.89
12	**75.5±1.11**	**50.0±1.46**	**71.1±2.92**	**73.8±0.41**
11	195.4±0.92	137.5±2.2	107.2±0.80	117.0±3.60
10	298.0±2.79	235.9±4.91	127.7±0.7	135.8±1.21

*Particle sizes in nm measured as M±SD are showed. Oil/Surf ratio (Oil to Surfactant ratio).

2) Polydispersion index.

Table II shows the results obtained from the polydispersion index (PDI) which is a parameter indicating the homogeneity of the particle size in the emulsions formulated to different HLBs and concentrations (1:1, 1:1.5, 1:2, 1:3 v/v) of rosemary essential oil:surfactant ratio. The formulation with HLB 12 at concentration 1:1.5 shows a PDI of 0.204, obtaining the highest PDI in the HLB 13 at concentration 1:2, with a value of 0.725 (Table II). This parameter is important in the characterization of emulsions; a PDI in a range between 0.2-0.5 is synonymous of stability. However, a PDI greater than 0.5, instability phenomena such as flocculation, Ostwald maturation, sedimentation or creaming may occur [20].

TABLE II. EFFECT OF HLB VALUE AND SURFACTANT CONCENTRATION ON THE POLYDISPERSION INDEX

Oil/Surf ratio (wt/wt) HLB	**Polydispersion Index (PDI)**			
	1:1	***1:1.5***	***1:2***	***1:3***
14	0.407±0.025	0.566±0.125	0.308±0.049	0.480±0.045
13	0.449±0.016	0.271±0.01	0.725±0.016	0.309±0.015
12	**0.320±0.013**	**0.204±0.01**	**0.424±0.058**	**0.281±0.015**
11	0.211±0.006	0.248±0.004	0.338±0.003	0.371±0.027
10	0.333±0.007	0.271±0.001	0.260±0.000	0.241±0.005

*The PDI values measured as M±SD are showed. Oil/Surf ratio (Oil to Surfactant ratio).

According to the obtained results, the most acceptable nanoemulsion is that obtained to HLB 12, concentration 1:1.5

(Tables I and II). These results are similar to obtained by Mostafa & cols., which obtained nanoemulsions from Cumin essential oil elaborated to HLB 16.7, a particle size of 69 nm and a PDI of 0.23 [21], confirming the stability of the processed emulsions.

3) Zeta-Potential.

Table III shows that all the emulsions are negatively charged between the range of -15.1 to -30.7 mV. The surfactants used in this study are nonionic surfactants that should not present any charge [22]. However, some studies that shown emulsions stabilized with nonionic surfactants may be charged, which can be due to the presence of ionizable surface impurities (such as fatty acids) or the adsorption of hydroxyl ions (OH^-) or hydrogen ions (H^+). This phenomenon is pH-dependent [11]. According to the particle size and the PDI parameters, the emulsion of greatest interest is the emulsion designed with HLB 12, concentration 1:1.5, which obtained a zeta-potential of -26.70 mV.

TABLE III. ZETA-POTENCIAL IN RELATION TO HLB.

Oil/Surf ratio (wt/wt) HLB	**Zeta-potential (mV)**			
	1:1	***1:1.5***	***1:2***	***1:3***
14	-15.1±0.60	-24.0±0.37	-22.2±1.15	-24.0±2.34
13	-23.3±1.33	-19.9±1.24	-23.8±4.42	-22.7±1.33
12	**-17.7±2.60**	**-26.7±1.13**	**-23.1±1.15**	**-23.1±0.71**
11	-19.2±0.81	-32.2±2.51	-28.1±2.32	-27.7±1.95
10	-26.3±0.29	-28.2±0.50	-30.7±0.95	-30.0±0.21

*Zeta-potential values measured as M±SD are showed. Oil/Surf ratio (Oil to Surfactant ratio).

Zeta-potential is an electrostatic measure that can give information about the physicochemical stability of a nanoemulsion. Therefore, it determines how much repulsion there is between the particles of the colloidal system. This parameter is essential for the design of nanoemulsions since the particles needed electrical charge repulsions to avoid aggregation phenomena that destabilize the system. It has been reported that the optimal value for electrostatic stabilization of the colloidal system is a zeta-potential between 30 and 60 mV, so, zeta-potentials between 5 and 15 mV, indicates limited flocculation, and, between 3 and 5 mV, maximum flocculation [23]. Mostafa & cols. obtained zeta-potentials in a range between -8 and -33 mV in nanoemulsions of cumin essential oil with an HLB of 16.7, which, according to the range obtained, were defined as stable [21]. For that reason, the emulsion with HLB 12, 1:1.5 oil: surfactant ratio, has an acceptable zeta-potential, which can confer good stability on the nanoemulsion.

IV. CONCLUSSION

This study confirmed that rosemary essential oil can be effectively encapsulated within food-grade nanoemulsions stabilized by nonionic surfactants.

Optimization of formulation showed that nanoemulsion with HLB 12, 1: 1.5 oil to surfactant ratio and 10 min sonication time, is the optimum formulation condition because of the small particle size (50 nm), good homogeneity, measured as polydispersion index (0.204), and stability (zeta-potential of 26.7).

Nanoemulsions obtained can be considered as stable systems and be used for application within food, beverage and pharmaceutical products.

REFERENCES

[1] Bušić A, Komes D, Belščak-Cvitanović A, Vojvodić Cebin A, Špoljarić I, Mršić G, Miao S. The Potential of Combined Emulsification and Spray Drying Techniques for Encapsulation of Polyphenols from Rosemary (*Rosmarinus officinalis* L.) Leaves. Food Technol Biotechnol. 2018 Dec;56(4):494-505. doi: 10.17113/ftb.56.04.18.5680.

[2] Loussouarn M, Krieger-Liszkay A, Svilar L, Bily A, Birtić S, Havaux M. Carnosic Acid and Carnosol, Two Major Antioxidants of Rosemary, Act through Different Mechanisms. Plant Physiol. 2017 Nov;175(3):1381-1394. doi: 10.1104/pp.17.01183. Epub 2017 Sep 15.

[3] Erkan N, Ayranci G, Ayranci E. Antioxidant activities of rosemary (Rosmarinus Officinalis L.) extract, blackseed (Nigella sativa L.) essential oil, carnosic acid, rosmarinic acid and sesamol. Food Chem. 2008 Sep 1;110(1):76-82. doi: 10.1016/j.foodchem.2008.01.058. Epub 2008 Feb 6.

[4] Altinier G, Sosa S, Aquino RP, Mencherini T, Della Loggia R, Tubaro A. Characterization of topical antiinflammatory compounds in Rosmarinus officinalis L. J Agric Food Chem. 2007 Mar 7;55(5):1718-23. Epub 2007 Feb 9.

[5] Poeckela D, Greinera C, Verhoffa M, Raub O, Tauschb L, Hörnigb C, Steinhilberb D, Schubert-Zsilaveczb M, Werza O. Carnosic acid and carnosol potently inhibit human 5-lipoxygenase and suppress pro-inflammatory responses of stimulated human polymorphonuclear leukocytes. Biochem Pharmacol. 2008 Jul 1;76(1):91-7. doi: 10.1016/j.bcp.2008.04.013. Epub 2008 May 1.

[6] Dörrie J, Sapala K, Zunino SJ. Carnosol-induced apoptosis and downregulation of Bcl-2 in B-lineage leukemia cells. Cancer Lett. 2001 Sep 10;170(1):33-9.

[7] Huang SC, Ho CT, Lin-Shiau SY, Lin JK. Carnosol inhibits the invasion of B16/F10 mouse melanoma cells by suppressing metalloproteinase-9 through down-regulating nuclear factor-kappa B and c-Jun. Biochem Pharmacol. 2005 Jan 15;69(2):221-32. Epub 2004 Nov 23.

[8] Visanji JM, Thompson DG, Padfield PJ. Induction of G2/M phase cell cycle arrest by carnosol and carnosic acid is associated with alteration of cyclin A and cyclin B1 levels. Cancer Lett. 2006 Jun 8;237(1):130-6. Epub 2005 Jul 14.

[9] Vergara D, Simeone P, Bettini S, Tinelli A, Valli L, Storelli C, Leo S, Santino A, Maffia M. Antitumor activity of the dietary diterpene carnosol against a panel of human cancer cell lines. Food Funct. 2014 Jun;5(6):1261-9. doi: 10.1039/c4fo00023d. Epub 2014 Apr 15.

[10] Baser K & Buchbauer, 2010. Handbook of essential oils. Boca Raton:CRC press Taylor & Francis Group.

[11] McClements DJ. 2005. Food emulsions: principles, practice, and techniques. 2nd Ed. Boca Raton: CRC Press.

[12] Tadros T, Izquierdo P, Esquena J, Solans C. Formation and stability of nano-emulsions. Adv Colloid Interface Sci. 2004 May 20;108-109:303-18.

[13] Jafari SM & McClements DJ. Nanotechnology Approaches for Increasing Nutrient Bioavailability. Adv Food Nutr Res. 2017;81:1-30. doi: 10.1016/bs.afnr.2016.12.008. Epub 2017 Jan 24.

[14] McClements DJ & Rao. 2011. Food-grade nanoemulsions: Formulation, fabrication, properties, performance, biological fate, and potential toxicity. Critical Reviews in Food Science and Nutrition 51: 285–330.

[15] Rašković A, Milanović I, Pavlović N, Ćebović T, Vukmirović S, Mikov M. Antioxidant activity of rosemary (Rosmarinus officinalis L.) essential oil and its hepatoprotective potential. BMC Complement Altern Med. 2014 Jul 7;14:225. doi: 10.1186/1472-6882-14-225.

[16] Al-Attar AM & Shawush NA. Physiological investigations on the effect of olive and rosemary leaves extracts in male rats exposed to thioacetamide. Saudi J Biol Sci. 2014 Nov;21(5):473-80. doi: 10.1016/j.sjbs.2014.08.004. Epub 2014 Sep 6.

[17] Walker R, Gumus, Decker & McClements, 2017. Improvements in the formation and stability of fish oil-in water nanoemulsions using carrier oils; MCT, thyme oil, & lemon oil, Journal of Food Engineering,

211, 60-68.

[18] Jo YJ, Chun JY, Kwon YJ, Min SG, Hong GP, Choi MJ. 2015. Physical and antimicrobial properties of trans-cinnamaldehyde nanoemulsions in water melon juice. LWT - Food Science and Technology, 60:444-451.

[19] Luchini A & Vitiello G. Understanding the Nano-bio Interfaces: Lipid-Coatings for Inorganic Nanoparticles as Promising Strategy for Biomedical Applications. Front Chem. 2019 May 15;7:343. doi: 10.3389/fchem.2019.00343. eCollection 2019. Review.

[20] Wu L, Zhang J y Watanabe W. 2011. Physical and chemical stability of drug nanoparticles. Advanced Drug Delivery Reviews, 63:456-469.

[21] Mostafa D, Kassem A, Asfour M, Al Okbi S, Mohamed D, Hamed T. 2015. Transdermal cumin essential oil nanoemulsions with potent antioxidant and hepatoprotective activities: In vitro and in vivo evaluation. Journal of Molecular liquids.212:pp. 6-15.

[22] Yang Y, Leser ME, Sher A, McClements DJ. (2013). Formation and stability of emulsions using a natural small molecule surfactant: Quillaja saponin (Q-Naturale®). *Food Hydrocolloids*, *30*(2), 589-596.

[23] Heurtault B, Saulnier P, Pech B, Proust JE, Benoit JP. Physico-chemical stability of colloidal lipid particles. Biomaterials. 2003 Oct;24(23):4283-300.

LWT - Food Science and Technology 118 (2020) 108694

Contents lists available at ScienceDirect

LWT - Food Science and Technology

journal homepage: www.elsevier.com/locate/lwt

In vitro and In vivo antioxidant properties of paprika carotenoids nanoemulsions

M.P. Jimenez-Escobar[a], L.I. Pascual-Mathey[b], C.I. Beristain[c], E. Flores-Andrade[d], M. Jiménez[c], L.A. Pascual-Pineda[c,*]

[a] Maestría en Ciencias Alimentarias, Universidad Veracruzana, Xalapa, 91000, Veracruz, Mexico
[b] Facultad de QFB, Universidad Veracruzana, Xalapa, Veracruz, 91000, Mexico
[c] Centro de Invesigación y Desarrollo en Alimentos (CIDEA), Universidad Veracruzana, Xalapa, Veracruz, 91000, Mexico
[d] Facultad de Ciencias Químicas de la Universidad Veracruzana, Orizaba, Veracruz, Mexico

ARTICLE INFO

Keywords:
Carotenoids nanoemulsions
Surfactant
Transaminase activity
Antioxidant properties

Chemical compounds studied in this article:
Paprika oleoresin
(PubChem CID: 11980947)
DPPH
(PubChem CID: 2735032)
Trolox
(PubChem CID: 40634)
TPTZ
(PubChem CID: 77258)
Tween 40
(PubChem CID: 92329579)
Methanol
(PubChem CID: 887)
Ferric chloride
(PubChem CID: 24380)
Pentobarbital
(PubChem CID: 4737)
Sodium deoxycholate
(PubChem CID: 23668196)
Sodium chloride
(PubChem CID: 5234)

ABSTRACT

This study aimed to investigate the protective role of emulsions loaded with paprika oleoresin carotenoids on liver and serum of healthy rats. Additionally, the study explored the effects of nonionic surfactants on the liver, which have not been reported. Conventional (CE) and nano (NE) emulsions were prepared and characterized, showing particle size of 157.9 and 39.2 nm, respectively and a monodisperse-size distribution. Carotenoid concentration analyzed by the DPPH method (EC_{50}) were 347 and 359 μg/mL for CE and NE, respectively. Both emulsions and the surfactant alone (Tween 40) were orally administered to Wistar rats. The results obtained in this study suggests that carotenoid emulsions have a protective effect on liver due to an increase of antioxidant activity, without modifying the transaminases activity. However, when the surfactant was administered alone, a damage on the liver was observed. The damage observed indicates that it is necessary to analyze the appropriate surfactant when emulsions and nanoemulsions are designed.

1. Introduction

Paprika oleoresin is a lipid solution from ripe fruits of *Capsicum annuum* L., an excellent source of carotenoid pigments. Carotenoids have known to have a role in maintaining health and prevention of diseases by acting as an antioxidant, protecting cells and tissues against damaging reactive oxygen species (ROS). They present high free-radical scavenging properties; associated to their multiple conjugated double bonds. However, this structural characteristic makes them sensitive to O_2, light, and heat, resulting in the loss of their functionality (Woodall, Lee, Weesie, Jackson, & Britton, 1997). Additionally, carotenoids are insoluble in water, which significantly limits their application in food

* Corresponding author. Centro de Invesigación y Desarrollo en Alimentos (CIDEA), Universidad Veracruzana, Dr. Luis Castelazo Ayala s/n Col. Industrial Ánimas, C.P. 91190, Xalapa, Veracruz, Mexico.
E-mail addresses: lupascual@uv.mx (L.I. Pascual-Mathey), cberistain@uv.mx (C.I. Beristain), enflores@uv.mx (E. Flores-Andrade), maribjimenez@uv.mx (M. Jiménez), lpascual@uv.mx (L.A. Pascual-Pineda).

https://doi.org/10.1016/j.lwt.2019.108694
Received 17 January 2019; Received in revised form 19 September 2019; Accepted 25 September 2019
Available online 26 September 2019
0023-6438/

formulations and both nutraceutical and pharmaceutical products. Furthermore, crystalline structures of carotenoids are often poorly absorbed in the intestine (Kiokias & Gordon, 2004). Oil-in-water emulsions and nano-emulsions with carotenoids in the dispersed oil phase are promising delivery systems to improve their bioavailability. Previous studies have shown the parameters that modify the bioaccessibility or bioavailability of carotenoids incorporated within nanoemulsion-based delivery systems. These studies focused on the oil type (medium chain triglyceride to long-chain triglyceride) (Salvia-Trujillo, Qian, Martin-Belloso, & McClements, 2013), particle size (Wang, Liu, Mei, Nakajima, & Yin, 2012), interfacial structure (Liu, Hou, Lei, Chang, & Gao, 2012), and use of emulsifiers improving functional attributes by conjugating proteins, polysaccharides or polyphenols (Liu, Ma, McClements, & Gao, 2016). However, the mechanisms through which the absorption is improved, have not been fully understood.

The design of the emulsion should provide specific performance in the gastrointestinal tract. It is important that the oil droplets in the emulsions be fully covered with the emulsifier in order to protect bioactive molecules from degradation during digestion. Nevertheless, an excess in the number of surfactant molecules can cause destabilization in the system and lead to degradation of bioactive molecules (Pascual-Pineda, Flores-Andrade, Jiménez-Fernández, & Beristain, 2015) as well as their accumulation in secondary target organs after administration (Brenner et al., 2018). Hence, the evaluation of some biomarkers in specific tissues is critical when nanoparticles are administered. In this sense, transaminases are the most sensitive biomarkers for hepatic disease and myocardial infarction, since the presence of elevated levels of transaminases is involved in the cellular damage and toxicity (Yousef, Saad, & El-Shennawy, 2009). It is essential to know if non-ionic surfactants have possible health effects as they are ingested, either absorbed at the interfacial layer or free in the continuous phase of emulsions. As far as we are concern, there have been no reports of *in vivo* systems, on the protection role of paprika carotenoids emulsions, nor on the effect of the excess of surfactant non-interacting at the interface. Therefore, the objective of this work was to evaluate the antioxidant and physicochemical properties of paprika oleoresin carotenoids loaded into conventional and nano-emulsions, as well as the effect of the surfactant used on the antioxidant capacity and the level of transaminases activity, employing an *in vivo* model.

2. Materials and methods

2.1. Materials

Paprika oleoresin of 100,000 color units (2500 ASTA) was obtained from AMCO Company (Mexico City). 2,2-Diphenyl-1-picrylhydrazyl (DPPH), Trolox (6-hydroxy-2,5,7,8-tetramethylchroman-2-carboxylic acid), 2,4,6- Tris(2-pyridyl)-1,3,5-triazine (TPTZ) and Tween 40 were purchased from Sigma Chemical Company (St. Louis, MO, USA).

All chemicals, including Tween 40 were purchased from Sigma Chemical Company (St. Louis, MO, USA) and all other chemicals used were of analytical grade.

2.2. Animals

Twenty Wistar male rats, 21-weeks old with body weights between 400 and 600 g were used. Rats were maintained at room temperature under standard laboratory conditions (12:12 h light-dark cycle; noise < 60 dB, and water and food access *ad libitum*) according to the guidelines of care and use of laboratory animals (Institute for Laboratory Animal Research, 2011), following the U.K. Animals (Scientific Procedures) Act, 1986 and associated guidelines and under the Norma Official Mexicana NOM-062-ZOO-1999. Animals were kept one week for adaptation before the beginning of experiments.

2.3. Preparation of conventional emulsion and nanoemulsion

Conventional emulsion (CE) and Nanoemulsion (NE) were prepared according to the highest stability criteria during storage (Pascual-Pineda et al., 2015) and the *in vitro* digestion (Pascual-Pineda et al., 2018). Emulsions were prepared using paprika oleoresin consist of mainly of vegetable oil (93%) as the disperse phase, Milli-Q water as the continuous phase and Tween 40 as the emulsifier. Emulsifier: paprika oleoresin ratio was 1:1 (wt/wt) in the emulsion system. The paprika oleoresin at 1% wt/wt was dispersed in aqueous Tween 40 surfactant solution at 1% wt/wt by using a high-speed homogenizer (Wiggen Hauser D-500; Berlin, Germany) at 4900 g and 40 °C for 10 min to obtain CE. NE was achieved by sonicating 20 mL of the CE through 250 W, 24 kHz high-power ultrasonicator (Branson Digital Sonifier; Danbury, CT, USA) at an amplitude of 65% for 10 min. A water-ice bath was used to maintain the temperature of the mixture at 30 ± 2 °C (Pascual-Pineda et al., 2015).

2.4. Experimental design

Experimental subjects were randomly assigned to four groups of five rats each. Animals in Group I (control) were administered orally with physiological saline solution (PISA). Group II (surfactant group) received surfactant dispersed in aqueous solution at a dose of 47.4 μg/kg/day orally, which was equivalent to the surfactant administered in carotenoids emulsion. The III and IV Groups were orally administered with 3 mg/kg/day of carotenoids loaded into CE and NE emulsions, respectively. All the experimental groups were administered twice per day, every 12 h, for 5 days through a displaceable sterilized intraesophageal stainless steel coupled to a disposable syringe. Body weight changes of rats were recorded during the experiment.

2.5. Emulsions characterization

2.5.1. Droplet size and polydispersity index measurements

Average particle size and polydispersity index (PDI) were evaluated with the Zeta-Sizer Nano ZS-2000 (Malvern Instruments, U.K) at 25 °C. Particle size was determined by dynamic light scattering at 643 nm and a scattering angle of 173°. Samples of 10 μL were diluted in 1000 μL of Milli-Q water to obtain a 1:100 dilution. The PDI was measured together with particle size in order to evaluate the homogeneity of the emulsions.

2.5.2. Carotenoids determination

Samples of 120 μL were dissolved in 25 mL of acetone, and the absorbance was measured using a spectrophotometer (Genesys™ 10S UV–Vis, Thermo Scientific, USA) at 472 and 508 nm. Absorbance values were introduced in the following equations to obtain the isochromic carotenoid fractions (Hornero-Méndez & Minguez-Mosquera, 2001):

$$C^R = \frac{A_{508} \text{ x } 2144.0 - A_{472} \text{ x } 403.3}{270.9} \quad (1)$$

$$C^Y = \frac{A_{472} \text{ x } 1724.3 - A_{508} \text{ x } 2450.1}{270.9} \quad (2)$$

$$C^T = C^R + C^Y \quad (3)$$

where C^R, C^Y and C^T were the red, yellow and total fractions (μg/mL), respectively, and A was the absorbance of the sample.

2.5.3. Determinations of antioxidant activity

In the DPPH assay samples were diluted with distilled water to obtain theoretical carotenoids concentrations ranging from 60 to 600 μg/mL. A volume of 2.95 mL of 0.061 mmol/L of DPPH methanol solution was mixed with 50 μL of the diluted emulsions. The absorbance was measured at 517 nm after 30 min at 25 °C in the dark with a spectrophotometer (Genesys™ 10S UV–Vis, Thermo Scientific, USA).

The control contained methanol (98% v/v) instead of the emulsion while the blank contained methanol instead of DPPH solution. The scavenging of DPPH free radical activity was calculated by the following equation (Brand-Williams, Cuvelier, & Berset, 1995):

$$Scavenging\ DPPH\ free\ radial\ percentage(\%) = \left(\frac{1 - A_{sample} - A_{blank}}{A_{control}}\right) * 100 \quad (4)$$

where A is the absorbance using the sample, blank or control. The scavenging percentage was plotted against the concentration of the samples, and the half maximal effective concentration (EC_{50}) value was determined by a linear regression analysis.

2.5.4. Ferric reducing antioxidant power (FRAP) assay

The ferric reducing antioxidant capacity (FRAP) assay was carried out as previously described (Benzie & Strain, 1996) with some minor modifications. The FRAP solution was freshly prepared on the day of use, by mixing acetate buffer (pH 3.6), ferric chloride solution (20 mmol) and TPTZ solution (10 mmol TPTZ in 40 mmol HCl) in a proportion of 10:1:1, respectively. Following, 3 mL of FRAP solution were incubated protected from light at 37 °C with 375 μL of distilled water and 25 μL of sample for 30 min. Absorbance was recorded at 593 nm using a spectrophotometer. The control sample was prepared by mixing 400 μL distilled water and 3 mL FRAP solution. The Trolox standard curve was used to calculate the antioxidant activity of the samples in relation to Trolox and was expressed as μmol of Trolox equivalents per mL of sample.

2.6. Blood and liver samples processing

Rats were euthanized with an overdose of pentobarbital (50 mg/kg, Pisabental, PiSA) after fasting for 12 h. Blood samples were collected by cardiac puncture and centrifuged at 2852 g for 5 min at 4 °C to obtain the serum and stored at −20 °C for further analysis. The color of livers was measured with a colorimeter (ColorFlex V1-72 SNHCX 1115 Hunter Lab, USA) using parameters L*, a*, and b* values, and the hue angle (H °) was the arctan(b*/a*).

Liver tissues were homogenized in RIPA Lysis Buffer (TRIS 50 mM, NaCl 150 mM, SDS 0.1%, sodium deoxycholate 0.5%, NP-40 0.5% and PMSF 1%) and protease inhibitor cocktail tablets (ROCHE), previous powder of samples in liquid nitrogen. The lysates were incubated for 1 h at 4 °C in constant agitation and centrifuged at 4105 g for 30 min at 4 °C to obtain supernatants. The FRAP test was used for the determination of the antioxidant activity of serum and liver. In the FRAP test, the reaction mixture (10 μL of sample, 30 μL of distilled water and 300 μL of FRAP reagent) was maintained in the dark at 37 °C for 30 min, the absorbance at 593 nm was then recorded using a Microplate reader (iMark TM, 1681130, Bio-rad, USA).

2.7. Serum aminotransferases quantification

The alanine aminotransferase (ALT) and aspartate aminotransferase (AST) levels were measured spectrophotometrically at 340 nm in serum using commercial kits (Spinreact, Spain, refs: ALT-1001172, AST-1001162).

2.8. Statistical analysis

The experiments were performed at least in triplicate. One-way Analysis of Variance (ANOVA) for independent variables followed by the Tukey's test was carried out to obtain significant differences ($p < 0.05$) using the StatPlus:MacLE software. For each analysis, a significance level of 5% was assumed. The error bars presented on the figures correspond to the standard deviations.

Table 1
Physicochemical and antioxidant characteristics of paprika emulsions.

Characterization parameters	Emulsions	
	CE	NE
Particle size (nm)	157 ± 1.8[a]	39 ± 0.03[b]
PDI	0.268 ± 0.01[a]	0.228 ± 0.02[b]
Red fraction carotenoid content (μg/mL)	376 ± 10.5[a]	369 ± 9.4[a]
Yellow fraction carotenoid content (μg/mL)	243 ± 11.2[a]	236 ± 7.7[a]
Total carotenoid content (μg/mL)	623 ± 14.9[a]	607 ± 10.2[a]
FRAP (μmol Trolox/mL)	16.9 ± 0.51[a]	15.6 ± 0.50[b]
EC_{50} (μg/mL)	347 ± 12.6[a]	359 ± 5.9[a]

Different letters in the same row indicate significant differences among process (Tukey's test, α = 0.05).

3. Results and discussion

3.1. In vitro study

Table 1 shows the physicochemical characterization of the emulsified paprika oleoresin. The particle size of CE emulsion was 157 ± 1.8 nm with a polydispersity index of 0.26 ± 0.01, whereas the particle size of NE was 39 ± 1.8 nm with a PDI of 0.22 ± 0.02. These results suggested that the surfactant (Tween 40) can be used to obtained emulsions in the nanometric range. Our results showed that the ultrasonic process produces a narrower particle distribution. Before sonication, the sample was optically opaque, which turned to optically transparent after sonication (Fig. 1). The transparent emulsions are preferable for applications in liquid food because the optical appearance of the products is minimally affected. Additionally, it has been shown that when bioactive molecules encapsulated within lipid droplets, the bioavailability of highly lipophilic functional molecules, increases as the droplet size decreases (Kesisoglou, Panmai, & Wu, 2007).

The total carotenoid content and antioxidant activity of the nanoemulsion was slightly lower than that of the conventional emulsion; however, there was no significant difference between the carotenoids content of both emulsions (Table 1). The total antioxidant activity of emulsion and nanoemulsion was 16.90 ± 0.51 and

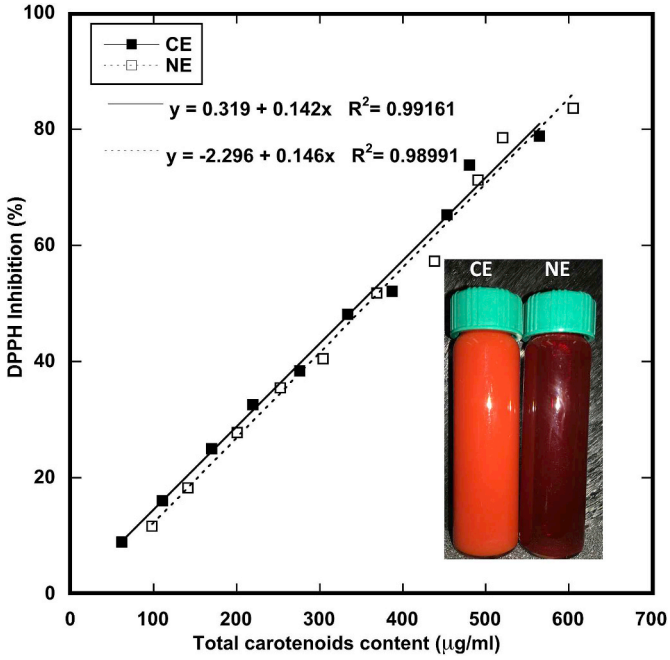

Fig. 1. Effect of total carotenoid concentration of paprika on scavenging DPPH activity percentage of conventional (■) and nanoemulsions (□). Lines represent a linear regression analysis of the experimental data points. (Inset) Pictures from visual observation of conventional and nanoemulsions.

15.61 ± 0.50 μmol Trolox equivalents/mL in the FRAP assay, respectively. The results showed that values of the emulsified paprika oleoresin where similar or higher than those values observed for some fruits juices such as blueberry juice (17.8–3.6 μmol Trolox equivalents/g) (Kraujalyte, Venskutonis, Pukalskas, Česoniene, & Daubaras, 2015) and black carrot juice (23 ± 2 μmol Trolox equivalents/mL of juice), which was considered exceptionally high. Fig. 1 depicts the effect of carotenoids concentration loaded in CE and NE emulsions on the antioxidant potential measured by the DPPH assay. Both emulsions exhibited a linear increase in the percentage of scavenging DPPH activity as the total carotenoid content was increased. The parameters of the linear equations and the goodness of fit can also be observed in Fig. 1. Therefore, the antioxidant activity in the emulsions was directly related to the carotenoids present in the paprika oleoresin, mostly capsanthin and capsorubin, which were responsible of the intense red color in paprika (Kim, Park, & Hwang, 2004). In the DPPH assay, the EC_{50} values were 347 and 359 μg/mL for CE and NE, respectively. These results confirm a slight decrease in the nanoemulsion antioxidant capacity. Our results were higher than those found in curcumin and tocopherol nanoemulsions with EC_{50} values of 118 and 109 μg/mL, respectively (Nikolic et al., 2018). The lower antioxidant activity for nanoemulsion can be attributed to an increase of both, oxygen accessibility and free-radicals dissolved in the continuous phase generated in the cavitation process (Chandrapala, Oliver, Kentish, & Ashokkumar, 2012). The slight decrease in antioxidant activity in the NE was due to an increase in the interfacial area and a reduction of the particle size. Such interactions may lead to the degradation of carotenoids, or other antioxidants present in the paprika oleoresin because they are sensitive to heat, light, and oxidative reactions (Woodall et al., 1997). Similar results were obtained by Ha et al. (2015) for nanoemulsions of lycopene-enriched tomato extract. They found that the droplets smaller than 100 nm exhibited lower antioxidant activity than those with sizes between 100 and 200 nm.

3.2. In vivo study

Fig. 2 shows the percentage of body weight changes after the treatment of the different groups. The positive control group showed a slight weight gain. Nevertheless, a weight loss of 14% in the surfactant group was observed, whereas for CE and NE, groups the weight loss was 7 and 8% respectively. Some authors have considered the body weight loss as an important indicator of toxicity (Amin, Abdel Hameid, & Abd Elsttar, 2010). Weight loss has been related to the formation of free-radicals leading to oxidative stress and activity inhibition of antioxidant enzymes glutathione peroxidase, superoxide dismutase and, catalase. Moreover, a decrease in antioxidant enzymes was also observed when a xenobiotic or other agents were administered, i.e., cisplatin (Atessahin, Yilmaz, Karahan, Ceribasi, & Karaoglu, 2005), and chronic ethanol (Kasdallah-Grissa et al., 2007).

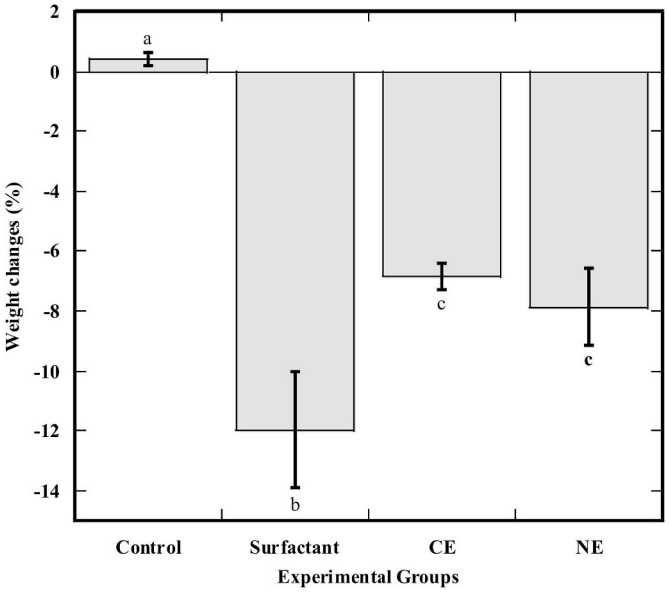

Fig. 2. Percentage body weight of experimental rats administered with 47.4 μg/kg/day of surfactant, and 3 mg/kg/day of carotenoids of paprika loaded into conventional (CE) and nanoemulsions (NE) over the experimental period. Error bars represent the standard deviation of six experiment rats. Letters represents significant different ($p < 0.05$).

Table 2
Antioxidant capacity measured by FRAP in serum and liver homogenates.

Experimental group	FRAP	
	Liver (μmol Trolox/g tissue)	Serum (μmol Trolox/mL)
Control	327 ± 0.2[a]	174 ± 16.0[a]
Surfactant	330 ± 5.5[a]	236 ± 13[b]
CE	346 ± 1.5[b]	271 ± 16.6[c]
NE	382 ± 9.8[c]	253 ± 12.1[bc]

Different letters in the same column indicate significant differences between experimental groups (Tukey's test, $\alpha = 0.05$).

On the other hand, the reduction of body weight observed in the CE and NE groups could be associated with a positive effect since the intake of *Capsicum annuum* L. reduced body weight and suppress body fat accumulation (Kawabata et al., 2006). Based on these considerations, it was necessary to study the oxidative stress in the experimental subjects.

Radical scavenging capacity in the experimental groups was determined in both, serum and liver using the FRAP assay. Table 2 shows that FRAP values were in the range of 327–382 μmol Trolox equivalents/g tissue and from 174 to 271 μmol Trolox equivalents/mL in liver and serum, respectively. Results showed that the highest antioxidant activity was found in the liver. This difference could be due to the highest biological antioxidant activity that occurs in the liver. The antioxidant activity values of our experiments were similar to those obtained in plasma and liver of Wistar male rats administered with freeze-dried and aqueous extract jaboticaba peels (Lenquiste et al., 2015), and in serum of mice administered with different kinds of wines (Gris et al., 2013). The highest antioxidant activity in the liver was also reported by Alía, Horcajo, Bravo, and Goya (2003) for rats with a diet rich in antioxidant dietary fiber from grapes. The percentage of increase or decrease of antioxidant activity normalized respect to the control group is shown in Fig. 3. The baseline represents the control group, and the height bars are proportional to the antioxidant activity. The FRAP percentages obtained in serum and liver from the animals administered with emulsified carotenoids and with pure surfactant showed higher values compared to those of the control group. However, an increase in antioxidant capacity in serum of subjects administered with emulsified carotenoids was observed. These results indicated that the emulsions were appropriate delivery vehicles to transport the carotenoids through the blood and liver. The subjects administered with CE (particle size higher than 100 nm) had 55% higher antioxidant activity in serum compared with that of the control group. Nevertheless, the nanoemulsion presented the maximum FRAP percentage in liver (17%). The lower size of NE allows the carotenoids within the drop to cross the cell membrane tissue and reach the liver more easily than those of the CE. It has been shown that when a nanoparticle drug delivery system is administered, nanocarriers inherently accumulate to high levels in the liver and spleen after injection (Brenner et al., 2018). This accumulation depends on particle size, shape, charge and surface functionality (Gustafson, Holt-Casper, Grainger, & Ghandehari, 2015). Therefore, the evaluation of some biomarkers is critical when nanoparticles are administered. Naturally, within the body, carotenoids absorption involves several steps: solubilization from the food matrix followed by micellization in the lumen, cellular uptake by intestinal mucosal cells, incorporation into chylomicrons and secretion of carotenoids and their

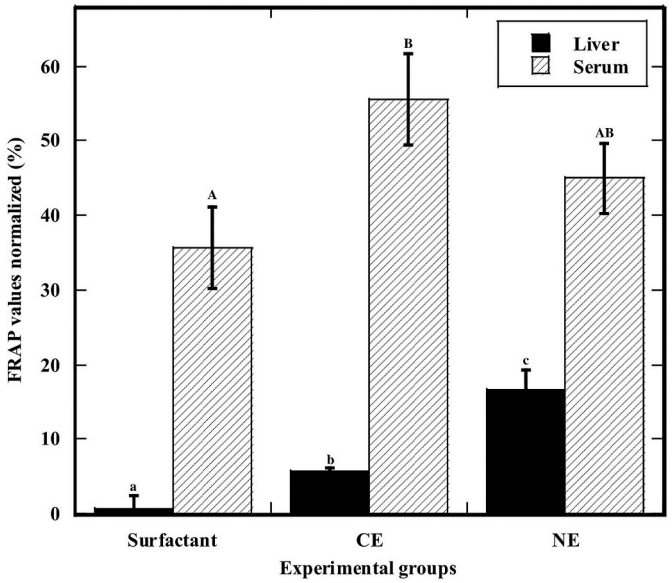

Fig. 3. Percent total of antioxidant activity in liver and of surfactant, conventional (CE) and nanoemulsion (NE) groups, each bar represents the mean of six subjects. The antioxidant activity was normalized respect to the control group.

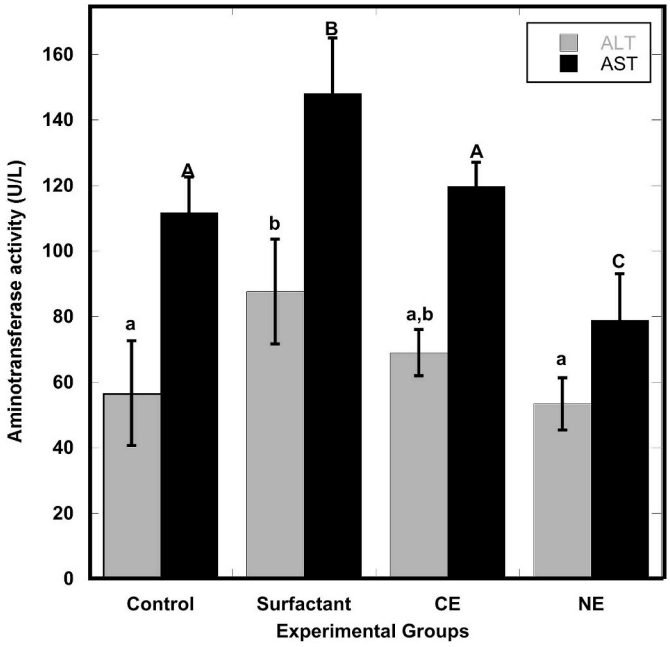

Fig. 4. Level of hepatic function markers in the surfactant, conventional emulsion (CE) and nanoemulsion (NE) groups. Error bars represent the standard deviation of six experiment rats. Letters represents significantly different ($p < 0.05$). AST (aspartate aminotransferase); ALT (alanine aminotransferase).

metabolites associated with chylomicrons into the lymph (Sanahuja et al., 2013). Carotenoids inside chylomicrons are transported into the lymphatic system and then, are incorporated into the lipoprotein in the liver and released into the bloodstream. Madkour and Abdel-Daim (2013) found that pre-treatment of albino Wistar rats with *Dunaliella salina* powder extract, which has great carotenoid content, showed a significant reduction of oxidative stress when compared to toxin treated group. They also reported the restoration of superoxide dismutase and total antioxidant capacity in the groups treated with 500 and 1000 mg/kg/$day_{d.w.}$ of *D. salina*. In this work, carotenoids were administered in a lower concentration (3 mg/kg/day); therefore, it is suggested that the emulsification process and the small particle size improve the emulsion bioavailability, showing an increase of the antioxidant activity.

Alanine aminotransferase (ALT) and aspartate transferase (AST) are biomarkers directly implicated in cellular damage and toxicity since they are released from the liver into the circulatory system after cellular damage (Yousef et al., 2009). ALT is more specific for detecting liver injury, whereas AST is also released in cardiac and muscle injury (Madkour & Abdel-Daim, 2013). The activity of liver ALT and AST enzymes is shown in Fig. 4. In the subjects treated with emulsified carotenoids, serum levels of ALT and AST were not statistically different or were lower compared with the control group, which suggested that both, CE and NE, were safe at the used doses. This result agreed with that reported by Bitencourt et al. (2016), which showed no significant difference in AST and ALT levels in subjects administered with nanoparticles containing *Syzygium cumini* L. extract. In this study, an increase in AST and ALT levels of 32.3 and 54.9%, respectively was found for the surfactant-administered group. This correlates with the higher weight loss observed in rats from this group (Fig. 2). Several studies showed that chemicals, e.g., ethanol, carbon tetrachloride, paracetamol and thioacetamide, can lead to an increase in transaminases levels. In this sense, Kasdallah-Grissa et al. (2007) reported an increase in AST and ALT levels of 42 and 72%, respectively, for rats administered with ethanol. We found that Tween 40 promotes an increase of these biomarkers causing damage in the liver of the surfactant group. It is known that in a given solvent and above a critical concentration, the surface-active molecules organize themselves spontaneously into micellar aggregates. The surfactant solution above of the critical micelle concentration amphiphilic molecules may remain in three environments: disperse as monomers in the aqueous phase, forming aggregates (micelles), or adsorbed (as a film) at the air/water interface (Patist, Oh, Leung, & Shah, 2001). Since the surfactant molecules are not rigidly fixed in the micelle, they are in constant dynamic equilibrium with the monomers disperse in the aqueous phase (Mats, Franz, & Kerry Thomas, 1979), where they could be more susceptible to oxidative reactions. Kerwin (2008) reported that solutions of Tween 20 and 80 can undergo autoxidation and hydrolysis, leading to the formation of acids and hydroperoxides, which could influence the susceptibility to oxidative stress in rats. Hence, we suggest that the increase in transaminases levels is associated with the surfactant oxidative activity. It was observed that an increase of the interfacial area of NE causes a decrease in the AST and ALT activity because the surfactant molecules were interacting at the interface, and only fewer particles as monomers and micelles were dispersed into the systems.

The appearance and color of livers in the experimental groups together with parameters of luminosity (L^*) and hue angle (H°), are shown in Fig. 5. The L^* parameter indicates the luminosity of the sample which it was slightly higher for the control liver than for the livers of surfactant, CE and NE groups, showing no statistically significant differences among them. However, the photographs showed a pale red color and a clear necrotic region on the livers of the surfactant group. The hue angle is expressed in degrees and is a color measure, where red-orange-yellow corresponds to the range of 0 to 90°. In our work, the H° values were in the range of 18.7–29.2°, which corresponded to reddish hue. The livers of the groups treated with emulsified carotenoids (CE and NE) and surfactant had H° values significantly lower than the control group, where low hue angles are indicative of redness. The NE group show a H ° value of 22.55, which was similar to the control group in comparison with the CE and surfactant groups. The livers of the rats administered with emulsified carotenoids did not show a visual necrotic damage; this was also confirmed by the level of transaminases observed in this group. These results suggested that the surfactant not adsorbed at the interface causing damage and cell death (e.g., mitochondria, cell membrane, protein synthesis machinery and DNA). Therefore, the observed increase in AST levels could be associated with the necrosis resulting from mitochondrial damage caused by the administration of the surfactant. Conversely, this damage was

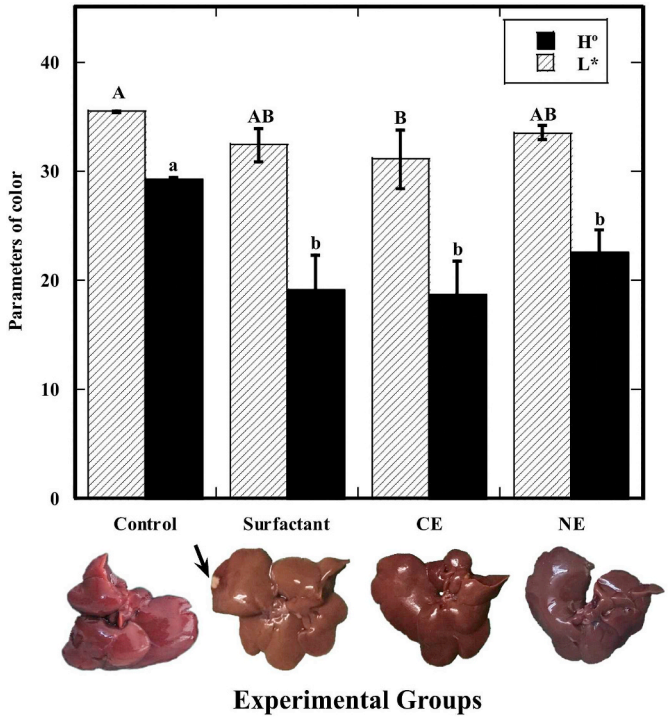

Fig. 5. Luminosity (*L**) and hue angle (H°) mean values and livers photographs of Wistar rats of the control, surfactant, conventional emulsion (CE) and nanoemulsion (NE) groups. (Inset). Visual photographs of rat livers.

not observed in the CE and NE emulsions, probably because the interaction of the surfactant at the interface, promotes the liver remains without damage.

4. Conclusion

CE and NE exhibited a linear correlation between antioxidant capacity and total carotenoid content. The *in vivo* study showed an increase in antioxidant capacity in the liver as the particle size decreases, without increasing the activity of transaminase enzymes. However, when the surfactant was administered in an aqueous solution, an increase in the activity of the transaminase enzymes was observed. When the non-ionic surfactant was administered and it was not adsorbed at the interface, it could cause liver damage, probably due to a mitochondrial injury that causes necrosis. These results suggested that it is necessary to analyze the appropriate surfactant when emulsions and nanoemulsions are designed. The results obtained in our study can be used to design food delivery systems to improve the bioaccessibility of lipophilic bioactive components.

Declaration of competing interest

All authors declare that they have no conflict of interest.

Acknowledgments

This work was carried out with the support of the Consejo Nacional de Ciencia y Tecnología (CONACyT), (CB-252692).

References

Alía, M., Horcajo, C., Bravo, L., & Goya, L. (2003). Effect of grape antioxidant dietary fiber on the total antioxidant capacity and the activity of liver antioxidant enzymes in rats. *Nutrition Research, 23*(9), 1251–1267. https://doi.org/10.1016/S0271-5317(03)00131-3.

Amin, K. A., Abdel Hameid, H., & Abd Elsttar, A. H. (2010). Effect of food azo dyes tartrazine and carmoisine on biochemical parameters related to renal, hepatic function and oxidative stress biomarkers in young male rats. *Food and Chemical Toxicology*. https://doi.org/10.1016/j.fct.2010.07.039.

Atessahin, A., Yilmaz, S., Karahan, I., Ceribasi, A. O., & Karaoglu, A. (2005). Effects of lycopene against cisplatin-induced nephrotoxicity and oxidative stress in rats. *Toxicology*. https://doi.org/10.1016/j.tox.2005.04.016.

Benzie, I. F. F., & Strain, J. J. (1996). The ferric reducing ability of plasma (FRAP) as a measure of "antioxidant power": The FRAP assay. *Analytical Biochemistry, 239*(1), 70–76. https://doi.org/10.1006/abio.1996.0292.

Bitencourt, P. E. R., Ferreira, L. M., Cargnelutti, L. O., Denardi, L., Boligon, A., Fleck, M., et al. (2016). A new biodegradable polymeric nanoparticle formulation containing Syzygium cumini: Phytochemical profile, antioxidant and antifungal activity and in vivo toxicity. *Industrial Crops and Products*. https://doi.org/10.1016/j.indcrop.2016.01.007.

Brand-Williams, W., Cuvelier, M. E., & Berset, C. (1995). Use of a free radical method to evaluate antioxidant activity. *Lebensmittel-Wissenschaft und -Technologie- Food Science and Technology, 28*(1), 25–30. https://doi.org/10.1016/S0023-6438(95)80008-5.

Brenner, J. S., Pan, D. C., Myerson, J. W., Marcos-Contreras, O. A., Villa, C. H., Patel, P., et al. (2018). Red blood cell-hitchhiking boosts delivery of nanocarriers to chosen organs by orders of magnitude. *Nature Communications*. https://doi.org/10.1038/s41467-018-05079-7.

Chandrapala, J., Oliver, C., Kentish, S., & Ashokkumar, M. (2012). Ultrasonics in food processing. *Ultrasonics Sonochemistry*. https://doi.org/10.1016/j.ultsonch.2012.01.010.

Gris, E. F., Mattivi, F., Ferreira, E. A., Vrhovsek, U., Filho, D. W., Pedrosa, R. C., et al. (2013). Phenolic profile and effect of regular consumption of Brazilian red wines on in vivo antioxidant activity. *Journal of Food Composition and Analysis*. https://doi.org/10.1016/j.jfca.2013.03.002.

Gustafson, H. H., Holt-Casper, D., Grainger, D. W., & Ghandehari, H. (2015). Nanoparticle uptake: The phagocyte problem. *Nano Today*. https://doi.org/10.1016/j.nantod.2015.06.006.

Ha, T. V. A., Kim, S., Choi, Y., Kwak, H. S., Lee, S. J., Wen, J., et al. (2015). Antioxidant activity and bioaccessibility of size-different nanoemulsions for lycopene-enriched tomato extract. *Food Chemistry, 178*, 115–121. https://doi.org/10.1016/j.foodchem.2015.01.048.

Hornero-Méndez, D., & Minguez-Mosquera, M. I. (2001). Rapid spectrophotometric determination of red and yellow isochromic carotenoid fractions in paprika and red pepper oleoresins. *Journal of Agricultural and Food Chemistry, 49*(8), 3584–3588. https://doi.org/10.1021/jf010400l.

Institute for Laboratory Animal Research (2011). *Guide for the care and use of laboratory animals* (8th ed.). Guide for the Care and Use of Laboratory Animalshttps://doi.org/10.2307/1525495.

Kasdallah-Grissa, A., Mornagui, B., Aouani, E., Hammami, M., El May, M., Gharbi, N., et al. (2007). Resveratrol, a red wine polyphenol, attenuates ethanol-induced oxidative stress in rat liver. *Life Sciences*. https://doi.org/10.1016/j.lfs.2006.11.044.

Kawabata, F., Inoue, N., Yazawa, S., Kawada, T., Inoue, K., & Fushiki, T. (2006). Effects of CH-19 sweet, a non-pungent cultivar of red pepper. *Decreasing the body weight and suppressing body fat accumulation by sympathetic nerve activation in humans*Bioscience, Biotechnology, and Biochemistryhttps://doi.org/10.1271/bbb.60206.

Kerwin, B. A. (2008). Polysorbates 20 and 80 used in the formulation of protein biotherapeutics: Structure and degradation pathways. *Journal of Pharmaceutical Sciences*. https://doi.org/10.1002/jps.21190.

Kesisoglou, F., Panmai, S., & Wu, Y. (2007). Application of nanoparticles in oral delivery of immediate release formulations. *Current Nanoscience, 3*(2), 183–190. https://doi.org/10.2174/157341307780619251.

Kim, S., Park, J., & Hwang, I. K. (2004). Composition of main carotenoids in Korean red pepper (Capsicum annuum, L.) and changes of pigment stability during the drying and storage process. *Journal of Food Science, 69*(1), FCT39–FCT44. https://doi.org/10.1111/j.1365-2621.2004.tb17853.x.

Kiokias, S., & Gordon, M. H. (2004). Antioxidant properties of carotenoids in vitro and in vivo. *Food Reviews International, 20*(2), 99–121. https://doi.org/10.1081/FRI-120037155.

Kraujalyte, V., Venskutonis, P. R., Pukalskas, A., Česoniene, L., & Daubaras, R. (2015). Antioxidant properties, phenolic composition and potentiometric sensor array evaluation of commercial and new blueberry (Vaccinium corymbosum) and bog blueberry (Vaccinium uliginosum) genotypes. *Food Chemistry*. https://doi.org/10.1016/j.foodchem.2015.05.031.

Lenquiste, S. A., Marineli, R. da S., Moraes, É. A., Dionísio, A. P., Brito, E. S. de, & Maróstica, M. R. (2015). Jaboticaba peel and jaboticaba peel aqueous extract shows in vitro and in vivo antioxidant properties in obesity model. *Food Research International*. https://doi.org/10.1016/j.foodres.2015.07.023.

Liu, Y., Hou, Z., Lei, F., Chang, Y., & Gao, Y. (2012). Investigation into the bioaccessibility and microstructure changes of B-carotene emulsions during in vitro digestion. *Innovative Food Science & Emerging Technologies, 15*, 86–95. https://doi.org/10.1016/j.ifset.2012.04.002.

Liu, F., Ma, C., McClements, D. J., & Gao, Y. (2016). Development of polyphenol-protein-polysaccharide ternary complexes as emulsifiers for nutraceutical emulsions: Impact on formation, stability, and bioaccessibility of ??-carotene emulsions. *Food Hydrocolloids, 61*, 578–588. https://doi.org/10.1016/j.foodhyd.2016.05.031.

Madkour, F. F., & Abdel-Daim, M. M. (2013). Hepatoprotective and antioxidant activity of Dunaliella salina in paracetamol-induced acute toxicity in rats. *Indian Journal of Pharmaceutical Sciences*. https://doi.org/10.4103/0250-474X.124747.

Mats, A., Franz, G., & Kerry Thomas, J. (1979). Dynamic and static aspects of solubilization of neutral arenes in ionic micellar solutions. *Journal of the American Chemical Society, 101*(2), 279–291. https://doi.org/10.1021/ja00496a001.

Nikolic, I., Jasmin Lunter, D., Randjelovic, D., Zugic, A., Tadic, V., Markovic, B., et al.

(2018). Curcumin-loaded low-energy nanoemulsions as a prototype of multi-functional vehicles for different administration routes: Physicochemical and in vitro peculiarities important for dermal application. *International Journal of Pharmaceutics, 550*(1–2), 333–346. https://doi.org/10.1016/j.ijpharm.2018.08.060.

Pascual-Pineda, L. A., Bautista-Hernández, S., Pascual-Mathey, L. I., Flores-Andrade, E., Jiménez, M., & Beristain, C. I. (2018). Development of paprika oleoresin dispersions for improving the bioaccessibility of carotenoids. *Revista Mexicana de Ingeniera Quimica, 17*(2), 767–776.

Pascual-Pineda, L. A., Flores-Andrade, E., Jiménez-Fernández, M., & Beristain, C. I. (2015). Kinetic and thermodynamic stability of paprika nanoemulsions. *International Journal of Food Science and Technology, 50*(5), 1174–1181. https://doi.org/10.1111/ijfs.12750.

Patist, A., Oh, S. G., Leung, R., & Shah, D. O. (2001). Kinetics of micellization: Its significance to technological processes. *Colloids and Surfaces A: Physicochemical and Engineering Aspects, 176*(1), 3–16. https://doi.org/10.1016/S0927-7757(00)00610-5.

Salvia-Trujillo, L., Qian, C., Martin-Belloso, O., & McClements, D. J. (2013). Influence of particle size on lipid digestion and β-carotene bioaccessibility in emulsions and nanoemulsions. *Food Chemistry, 141*(2), 1472–1480.

Sanahuja, G., Farré, G., Berman, J., Zorrilla-López, U., Twyman, R. M., Capell, T., et al. (2013). A question of balance: Achieving appropriate nutrient levels in biofortified staple crops. *Nutrition Research Reviews*. https://doi.org/10.1017/S0954422413000176.

Wang, P., Liu, H.-J., Mei, X.-Y., Nakajima, M., & Yin, L.-J. (2012). Preliminary study into the factors modulating β-carotene micelle formation in dispersions using an in vitro digestion model. *Food Hydrocolloids, 26*(2), 427–433.

Woodall, A. A., Lee, S. W. M., Weesie, R. J., Jackson, M. J., & Britton, G. (1997). Oxidation of carotenoids by free radicals: Relationship between structure and reactivity. *Biochimica et Biophysica Acta (BBA) - General Subjects, 1336*(1), 33–42. https://doi.org/10.1016/S0304-4165(97)00006-8.

Yousef, M. I., Saad, A. A., & El-Shennawy, L. K. (2009). Protective effect of grape seed proanthocyanidin extract against oxidative stress induced by cisplatin in rats. *Food and Chemical Toxicology*. https://doi.org/10.1016/j.fct.2009.02.007.

c-Fos immunoreactivity in the hypothalamus and reward system of young rats after social novelty exposure

Yvette M. Gómez-Gómez[a], Pedro Sánchez-Aparicio[d], Sara Mejía-Chávez[e], Fabio García-García[b], Luz I. Pascual-Mathey[c], Ulises Aguilera-Reyes[e], Oscar Galicia[f] and Arturo Venebra-Muñoz[e]

Socialization is an adaptive behavior during the early stages of life because it helps young animals become independent and determines healthy adult social behavior. Therefore, it is probable that the brain areas involved in the processing of social stimuli are more sensitive to social novelty during early life stages. To test this hypothesis, four groups of young male rats were exposed to different socioenvironmental stimuli; nonsocial physical novelty, social familiarity, social novelty, and a control group which received no stimulation. After stimuli exposure, brains were fixed and cut in coronal sections for c-Fos immunohistochemistry. The number of c-Fos-immunoreactive (c-Fos-ir) neurons in the paraventricular nucleus and supraoptic nucleus, the main producers of oxytocin and vasopressin, was compared, as well as in the nucleus accumbens and ventral pallidum, the main areas involved in reinforced behavior. A significantly higher number of c-Fos-ir neurons were found in animals exposed to social novelty in all areas, except in the supraoptic nucleus. In particular, the increase in c-Fos-ir in the paraventricular nucleus seems to be selective in response to social novelty, while the increase of c-Fos-ir in the nucleus accumbens and ventral pallidum suggests that social novelty during youth is a highly rewarding stimulus compared with social familiarity and nonsocial physical novelty. *NeuroReport* 30:510–515

NeuroReport 2019, **30**:510–515

Keywords: c-Fos, hypothalamus, nucleus accumbens, paraventricular nucleus, reward system, social novelty, supraoptic nucleus, ventral pallidum

[a]Neuroethology Institute, [b]Health Science Institute, [c]Faculty of Biological and Pharmaceutical Chemistry, Veracruzana University, Xalapa, [d]Faculty of Veterinary Medicine and Zootechnics, [e]Faculty of Science, Autonomous University of the State of Mexico, Toluca and [f]Department of Psychology, Iberoamericana University, Mexico City, Mexico

Correspondence to Arturo Venebra-Muñoz, PhD, Faculty of Science, Autonomous University of the State of Mexico, Instituto Literario 100, Col. Centro, 50000 Toluca, Mexico
Tel: +52 172 2296 5553; fax: +52 172 2296 5554;
e-mail: avenebram@uaemex.mx

Received 16 October 2018 **accepted** 8 March 2019

Introduction

At the behavioral level, a preference for social novelty compared with social familiarity and the nonsocial novelty, has been observed in adult rodents [1–4]. At the physiological level, it has been observed that, in adult male rats, the exposure to unknown young individuals induces a greater increase in the release of dopamine in the nucleus accumbens (Nacc) compared with rats exposed to familiar individuals [5]. Also, in human studies, it has been shown that the level of oxytocin in saliva increases during new social encounters, but not during familiar ones, possibly because it plays an anxiolytic role that helps to increase confidence between strangers [6].

Known as prosocial hormones, oxytocin and vasopressin are produced by the paraventricular nucleus (PVN) and supraoptic nucleus (SON) of the hypothalamus. Their participation in motivation associated with reproductive behaviors has been studied widely [7–9], but beyond their reproductive context, these hormones play a role in the transition from social novelty to familiarity and help create affective bonds by influencing the reward system. For example, on the one hand, it is well described that knockout rodents for oxytocin, vasopressin, or their receptor genes are incapable of creating new social memories [10,11]. On the other, it is well known that the reward system is necessary for learning, including social learning, and some of the brain structures that form part of the reward system are sensitive to oxytocin and/or vasopressin, among which are the Nacc and ventral pallidum (VP), areas known as hedonic hotspots because of their necessary activation for increasing 'liking' in response to reward. In this case, 'Liking' would help to reinforce coexistence between strangers and to form affective bonds [8,12].

Previous studies have reported the effect of enriched environments against the development of certain diseases, such as addictions, caused by an imbalance in the activity of the reward system [13]. Environmental enrichment comprises physical and social stimuli, which can be either familiar or new. These stimuli are applicated in young rats because youth is a sensitive window for brain plasticity. Although there is a lack of research of social novelty in young individuals, we think that social novelty is a strong stimulus that should be studied in enriched environments, taking into account its effects in the reward system. The social component in enriched environments is difficult to study; therefore, this study attempts to isolate the variables that can be found in enriched environments,

0959-4965 DOI: 10.1097/WNR.0000000000001236

emphasizing social novelty to observe its effects on the neuronal activity in specific areas of the reward system, and hypothalamic areas that produce oxytocin and vasopressin, using c-Fos as a marker of neuronal activity.

Methods

Subjects

Thirty-six male Wistar rats (*Rattus norvegicus*), aged between 28 and 30 days, were used. The specimens were obtained by controlled cross-breeding to ascertain their litter of provenance. Animal handling and internal bioterium conditions were applied in accordance with the official Mexican norm NOM-062-ZOO-1999 standards [14] and the *Guide for the care and use of laboratory animals* [15]. Every effort was made to minimize animals' discomfort. From postnatal day 11 onwards, males were gently handled for 2 min/day to habituate them to the experimenter. After weaning (postnatal day 21), males were separated by litter until postnatal day 28. Animals were divided into four groups: six rats in the control group (CG) received no type of stimulation, 10 rats were exposed to nonsocial physical novelty (PN), 10 rats were exposed to social familiarity (SF), and 10 rats were exposed to social novelty (SN).

Test area

Exposure to stimuli was carried out in polycarbonate cages (45 cm long, 25 cm wide and 20 cm high) with a metal mesh top (0.5 cm^2 cells) and a metal mesh (1.3 cm^2 cells) in the middle of the cage. The cage with the mesh represented a novel environment for the PN group, whereas for SF and SN groups, which were previously habituated to it, the mesh fulfilled the function to avoid body-to-body contact as well as behaviors like play and aggression but permitted olfaction and slight contact between the individuals. All tests were carried out during the first 4 h of dark, under red lighting.

Procedure for the control group

On postnatal day 28, rats were isolated individually for 48 h in standard bioterium cages (Fig. 1a), with food and water *ad libitum*, without any other type of stimulation. After this period, transcardial perfusion was performed for the fixation of the brain.

Procedure for the physical novelty group

Between postnatal days 28 and 30, rats were isolated individually in standard bioterium cages, with food and water *ad libitum*, without any other stimulation. After isolation, exposure tests were carried out. Rats were placed individually in the test cage for 30 min (Fig. 1b). After the tests, rats were isolated for 1 h before transcardial perfusion.

Procedure for the social familiarity group

Rats were isolated for a period of two days, from postnatal days 28–30. During both days, individual 1-h habituation sessions were conducted to familiarize the subjects with the test cage. Tests for this group were carried out in pairs, with five pairs formed with the condition that the rats were siblings and that they had been reared in the same litter. In the exposure tests, rats were placed on each side of the mesh and were left to interact for 30 min (Fig. 1c). After this period, animals were isolated individually for one hour before transcardial perfusion.

Fig. 1

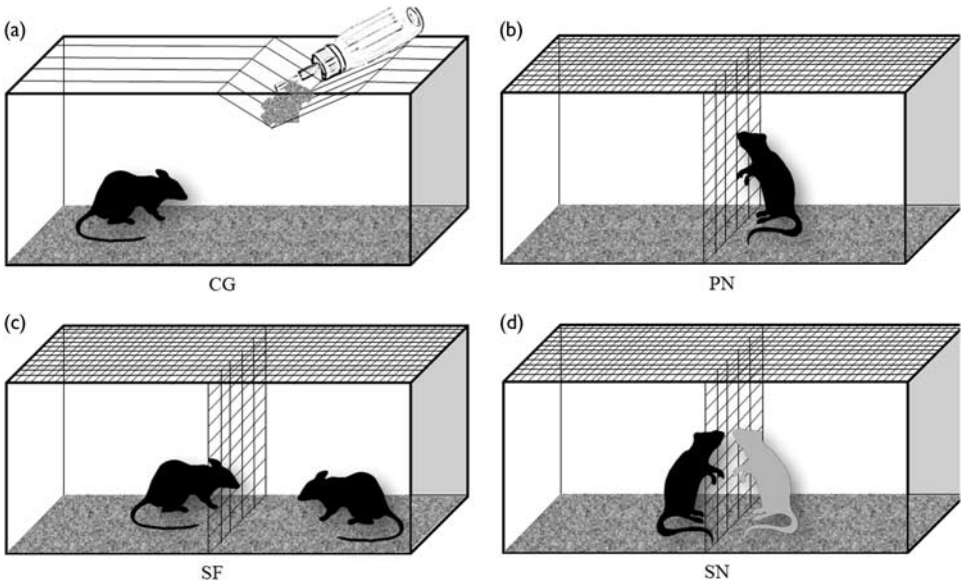

Diagrams of behavioral experiments. All animals were isolated for 48 h, including animals from the control group (CG) (a). After isolation, animals from the physical novelty (PN), social familiarity (SF), and social novelty (SN) groups were exposed to different stimuli for 30 min. Rats from the PN group were placed in the test cage individually (b); rats from the SF group were divided into pairs formed by siblings (c); and rats from the SN group were divided into pairs formed by nonsibling individuals born in different litters (d). The last two groups were previously habituated to the test cage.

Procedure for the social familiarity group

The procedure for this group was the same as for the SF group, except that pairs were formed with nonsibling rats from different litters (Fig. 1d).

Immunohistochemistry

Rats were deeply anesthetized intraperitoneally with sodium pentobarbital (40 mg/kg) and transcardial perfusion was carried out with saline solution (0.9%), followed by paraformaldehyde (4%) in 0.1 M PBS (pH 7.4) and sucrose (4%). Brains were removed and postfixed overnight, and then equilibrated to sucrose solutions of different gradients (10, 20, and 30%, 5 days each). Then, 40-μm coronal sections from the Nacc, core and shell (Bregma: 1.60–1.20 mm), VP (Bregma: 0.26 to −0.40 mm), PVN, and SON (Bregma: −1.30 to 1.60 mm) were obtained [16]. These brain regions were selected because they are involved in both the reward system and social interactions [11]. Briefly, tissue sections were incubated in 0.5% hydrogen peroxide for 10 min, and then incubated in PBS, 0.3% Triton X-100, and 3% normal goat serum for an hour. Then, tissue sections were incubated in the same solution with the addition of the c-Fos antibody (sc-52; Santa Cruz Biotechnology, Santa Cruz, California, USA) at a 1 : 250 dilution for two days at 4°C. For the secondary antibody (biotinylated goat anti-rabbit, sc-2040; Santa Cruz Biotechnology), a dilution of 1 : 250 was prepared in PBS with 0.3% Triton X-100, and tissue sections were incubated for 1 h at room temperature. The reaction was visualized with a solution of PBS with 0.06% diaminobenzidine, 1% nickel sulfate, and 1% cobalt chloride. Some sections from each experimental group were processed as described above, but without the primary antibody, as negative control groups for the immunohistochemistry.

Quantification of c-Fos-ir cells

c-Fos immunoreactivity was identified as a black-purple precipitate from the diaminobenzidine–nickel/cobalt reaction in the cell nucleus. All slides were coded and the c-Fos-ir

Fig. 2

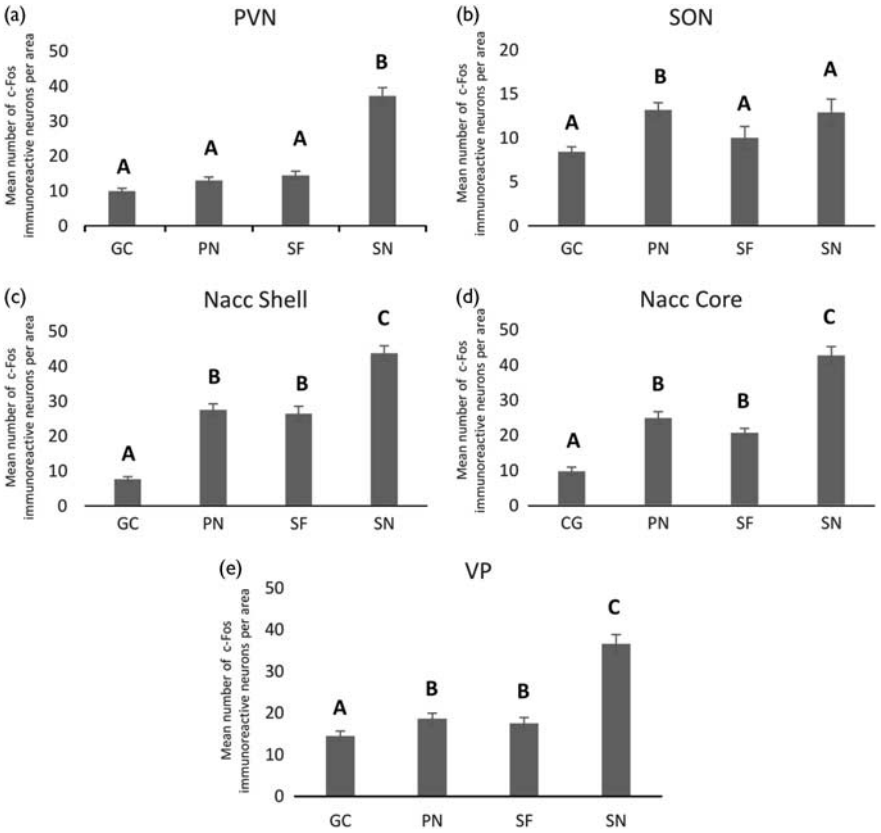

Immunohistochemistry analysis. The graphs show the average number of c-Fos-ir neurons in the different groups for each brain area ± SE; the letters A, B, and C above the bars indicate statistically significant differences in accordance to the Dunn test. Social novelty causes a higher number of c-Fos-ir neurons in the paraventricular nucleus (PVN) (a). The number of c-Fos-ir neurons in the supraoptic nucleus (SON) was higher in the PN group but only against CG; differences among the other groups were not statistically significant (b). In both regions of the nucleus accumbens (Nacc shell and core), the physical novelty (PN), social familiarity (SF), and social novelty (SN) groups presented a higher number of c-Fos-ir neurons than the control group (CG), but social novelty was the stimulus that induced a higher expression of c-Fos (c, d). The number of c-Fos-ir neurons in the ventral pallidum (VP) only increased significantly in response to social novelty (e). Nacc, nucleus accumbens; PN, physical novelty; PVN, paraventricular nucleus; SF, social familiarity; SN, social novelty; SON, supraoptic nucleus; VP, ventral pallidum.

Fig. 3

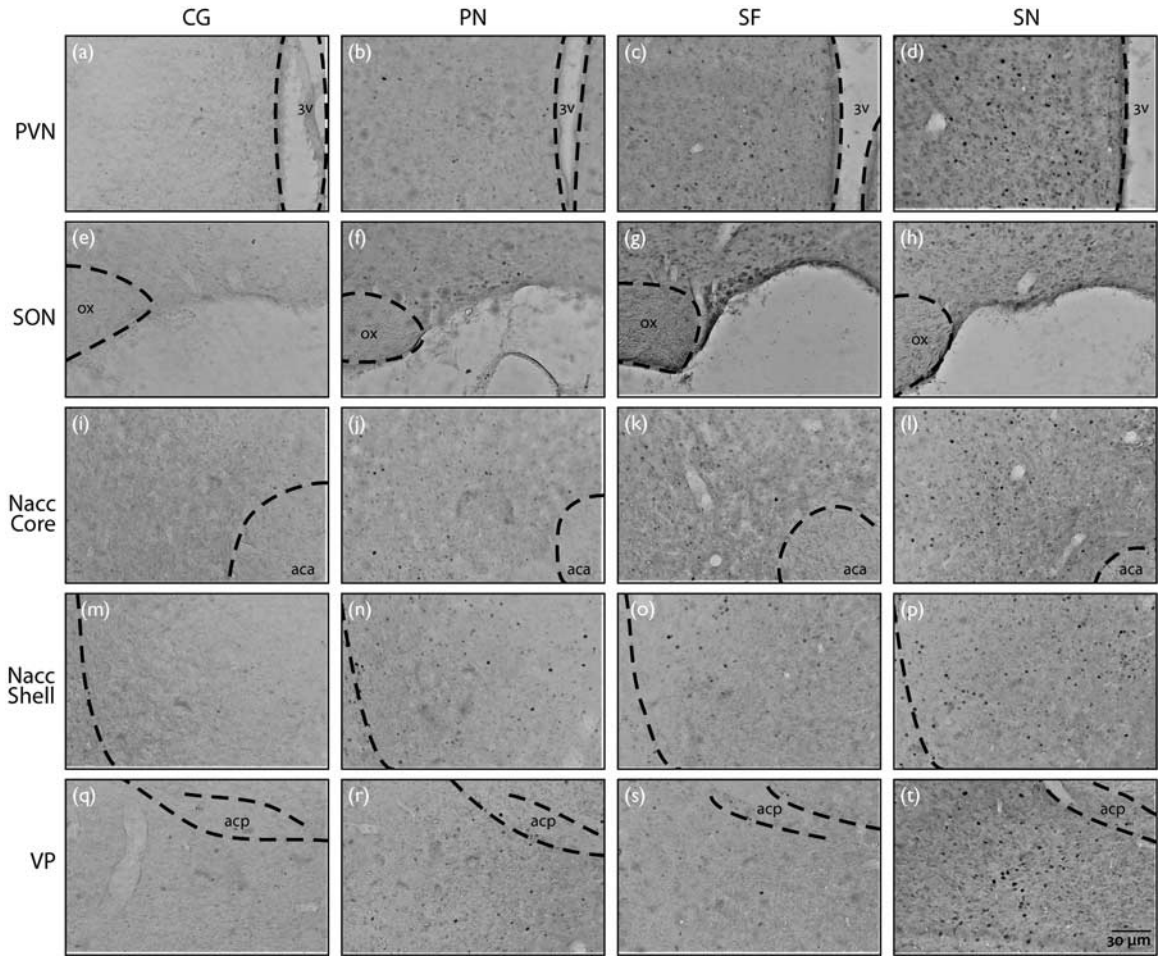

Microphotographs of the analyzed areas for the counting of c-Fos-ir neurons. Columns represent the different types of socioenvironmental stimuli (groups); rows represent the brain areas. Lowercase letters represent a specific area for a specific group: immunoreactivity of the four groups in PVN (a–d), SON (e–h), Nacc core (i–l), Nacc shell (m–p), and VP (q–t). In all areas, except the SON, a higher number of c-Fos-ir neurons can be observed clearly in the photographs of the SN group. The scale bar represents 30 µm for all photographs. Aca, anterior commissure anterior part; acp, anterior commissure-posterior part; CG, control group; Nacc, nucleus accumbens; ox, optic chiasm; PN, physical novelty; PVN, paraventricular nucleus; SF, social familiarity; SN, social novelty; SON, supraoptic nucleus; 3V, third ventricle; VP, ventral pallidum.

nuclei were counted in both hemispheres by two observers, blinded to experimental conditions and subjects, using an optic microscope with an ×40 objective (101 and 787 μm^2). Several sections per structure were analyzed using freeware imaging analysis (ImageJ; NIH, Bethesda, Maryland, USA) [13]. A Kruskal–Wallis test per area was applied to compare the experimental groups, and Dunn's tests were applied as post-hoc. Values were considered statistically significant at a P value of less than 0.05.

Results

Immunoreactivity in the hypothalamus

The number of c-Fos-ir neurons in the PVN and SON, the main producers of oxytocin and vasopressin, were counted. The number of neurons that expressed c-Fos in the PVN was higher in the SN group in comparison with the CG, PN, and SF groups (KW_{PVN}: $H_3 = 7.8147$, $P < 0.05$; (Figs 2a and 3a–d). The SON showed statistically significant differences in the numbers of c-Fos-ir neurons only between CG and PN groups (KW_{SON}: $H_3 = 7.8147$, $P < 0.05$); although a higher number of c-Fos-ir neurons was observed in the SF and SN groups, there were no statistically significant differences (Figs 2b and 3e–h).

Immunoreactivity in the reward system

The number of c-Fos-ir neurons was counted in the two areas that comprise the Nacc, shell and core, and in the VP. Compared with the CG, statistically significant differences were found in the core and shell in the PN, SF, and SN groups, with the SN being the group in which the highest number of c-Fos-ir neurons was found (KW_{Shell}: $H_3 = 7.8147$, $P < 0.05$; Figs 2d and 3m–p and KW_{Core}: $H_3 = 7.8147$, $P < 0.05$; Figs 2c and 3i–l). Also, compared with the other groups, the SN group presented a

statistically significant higher number of c-Fos-ir neurons in the VP (KW_{VP}: $H_3 = 7.8147$, $P < 0.05$; Figs 2e and 3q–t).

Discussion

Although previous studies have reported an increase in oxytocin in saliva during new social encounters between humans [6], no studies have reported whether the release of oxytocin in response to this type of encounter is produced by either the PVN or the SON. Although there is a long history of previous research on the importance of oxytocin and vasopressin during socialization [17–19], this is the first study that has carried out a comparison of the activity of both hypothalamic nuclei in response to various socioenvironmental contexts. The differences observed in the number of c-Fos-ir neurons of the hypothalamus suggest that the PVN could be the main supplier of oxytocin and, possibly, vasopressin during new social encounters because the expression of c-Fos increased significantly in response to the presence of an unfamiliar individual (Figs 2a and 3a–d) in contrast to the SON, in which no increase in c-Fos-ir neurons in response to social novelty was found (Figs 2b and 3e–h).

One of the reasons why the PVN has been studied more extensively than the SON is because of its broad connections to the reward system [9,20,21]. In nonreproductive contexts, oxytocin and vasopressin are involved in the formation of new social memories and the release of dopamine into the Nacc, mainly during new encounters in adult individuals [5,10,11]. According to the results of this research, the number of c-Fos-ir neurons increases in both the Nacc and VP in young individuals exposed to social novelty (Figs 2c–e and 3i–t). Studies have shown that the expression of c-Fos in the Nacc and VP could be influenced directly by other neurotransmitters, such as opioids and cannabinoids, as well as dopamine subsequent to exposure to various types of appetitive stimuli [22,23].

Given the results in this study, we suggest that the increased activity in these areas in response to social novelty could be caused directly by PVN oxytocin and vasopressin as the Nacc has oxytocin receptors and the VP has vasopressin receptors. It could also be attributed to the modulation of dopaminergic activity through the ventral tegmental area, given that this area also has oxytocin receptors [9,24].

The fact that social novelty induces a higher number of c-Fos-ir neurons in the Nacc and VP, which are considered hedonic hotspots because of their influence on the perception of pleasure [12], suggests that social novelty during youth is a highly rewarding stimulus, in comparison with other stimuli. Research in our laboratory is generally focused on the study of the influence of enriched environments on the propensity to addiction to commonly abused drugs such as nicotine [13]. Given the fact that addictions are directly related to the activity of the reward system, it is necessary to ascertain the environmental variables that may influence said system the most, like social novelty.

Having studied social novelty separately, we note that this variable may be the one with the most influence on the plasticity of the reward system induced by enriched environments; however, questions remain on the relationship of oxytocin, vasopressin, and the preference for social novelty in nonreproductive contexts, as well as the participation of other brain areas involved in the reward system, such as the ventral tegmental area, the amygdala, the hippocampus, and the prefrontal cortex.

Acknowledgements

Thanks are due to CONACYT for the scholarship awarded to Yvette M. Gómez-Gómez under reference number 478525.

Conflicts of interest

There are no conflicts of interest.

References

1 Van Loo PLP, Van de Weerd HA, Van Zutphen LFM, Baumans V. Preference for social contact versus environmental enrichment in male laboratory mice. *Lab Anim* 2004; **38**:178–188.
2 Moy SS, Nadler JJ, Perez A, Barbaro RP, Johns JM, Magnuson TR, *et al*. Sociability and preference for social novelty in five inbred strains: an approach to assess autistic-like behavior in mice. *Genes Brain Behav* 2005; **3**:287–302.
3 Peartree NA, Hood LE, Thiel KJ, Sanabria F, Pentkowsky NS, Chandler KN, *et al*. Limited physical contact through a mesh barrier is sufficient for social reward-conditioned place preference in adolescent male rats. *Physiol Behav* 2012; **105**:749–756.
4 Elliot BM, Grunber NE. Effects of social and physical enrichment on open field activity differ in male and female Sprague-Dawley rats. *Behav Brain Res* 2005; **165**:187–196.
5 De Leonibus E, Verheij MMM, Mele A, Cools A. Distinct kinds of novelty processing differentially increase extracellular dopamine in different brain regions. *Eur J Neurosci* 2006; **23**:1332–1340.
6 Tops M, Huffmeijer R, Linting M, Grewen KM, Light KC, Koole SL, *et al*. The role of oxytocin in familiarization habituation responses to social novelty. *Front Psychol* 2013; **4**:1–9.
7 Donalsdon ZR, Young LJ. Oxytocin, vasopressin and the neurogenetics of sociality. *Science* 2008; **322**:900–904.
8 Insel TR. Challenge of translation in social neuroscience: a review of oxytocin, vasopressin and affiliative behavior. *Neuron* 2010; **65**:768–779.
9 Love TM. Oxytocin, motivation and the role of dopamine. *Pharmacol Biochem Behav* 2014; **119**:49–60.
10 Ferguson JN, Young LJ, Hearn EF, Matzuk MM, Insel TR, Winslow JT. Social amnesia in mice lacking the oxytocin gene. *Nat Genet* 2000; **25**:284–289.
11 Bielsky IF, Hu SB, Szegda KL, Westphal H, Young LJ. Profound impairment in social recognition and reduction in anxiety-like behavior in vasopressin V1a receptor knockout mice. *Neuropsychopharmacology* 2004; **29**:483–493.
12 Berridge KC, Robbinson TE, Aldrige JW. Dissecting components of reward: 'liking', 'wanting' and learning. *Curr Opin Pharmacol* 2009; **9**:65–73.
13 Venebra-Muñoz A, Corona-Morales A, Santiago-García J, Malgarejo-Gutiérrez M, Caba M, García-García F. Enriched environment attenuates nicotine self-administration and induces changes in Δ-FosB expression in the rat prefrontal cortex and nucleus accumbens. *Neuroreport* 2014; **25**:688–692.
14 NORMA Oficial Mexicana: NOM-062-ZOO-1999. Especificaciones técnicas para la producción, cuidado y uso de los animales de laboratorio. Diario Oficial de la Federación [Official Mexican Norm: NOM-062-ZOO-1999. Technique specifications for the production, care and use of laboratory animals. Federation Official Journal]; 1999.
15 National Research Council. *Guide for the care and use of laboratory animals*. Washigton DC: National Academic Press; 2011.
16 Paxinos G, Watson C. *The rat brain in stereotaxic coordinates*. San Diego, CA: Elsevier Academic Press; 2005.
17 Lim MM, Young LJ. Vasopressin dependent neural circuits underlying pair bond formation in the monogamous prairie vole. *Neuroscience* 2004; **125**:35–45.

18 Shahrokh DK, Zhang TY, Dioro J, Gratton A, Meany MJ. Oxytocin dopamine interactions mediate variations in maternal behavior in the rat. *Endocrinology* 2010; **151**:2276–2286.
19 Ophir AG, Gessel A, Zheng DJ, Phelps SM. Oxytocin receptor density is associated with male mating tactics and social monogamy. *Horm Behav* 2012; **61**:445–453.
20 Buijs RM, De Vries GJ, Van Leeuwen FW. The distribution and synaptic release of oxytocin in the central nervous system. In: Amico JA, Robison AG, editors. *Oxytocin: clinical and laboratory studies*. Amsterdam: Excerpta Medica; 1985. pp. 77–86.
21 Sofronew MV. Projections from vasopressin, oxytocin and neurophysin neurons to neural targets in the rat and human. *J Histochem Cytochem* 1980; **28**:475–478.
22 Mahler SV, Smith KS, Berridge KC. Endocannabinoid hedonic hotspot for sensory pleasure: anandamide in nucleus accumbens shell enhances 'liking' of a sweet reward. *Neuropsychopharmacology* 2007; **32**:2267–2278.
23 Smith KS, Berridge KC. Opioid limbic circuit for reward: interaction between hedonic hotspots of nucleus accumbens and ventral pallidum. *J Neurosci* 2007; **27**:1594–1605.
24 Loup F, Tribollet E, Dubois-Dauphin M, Dreiffus JJ. Localization of high-affinity binding sites for oxytocin and vasopressin in the human brain. An autoradiographic study. *Brain Res* 1991; **555**:220–232.